

HYBRID ROCKET IGNITION SIMULATION AND EXPERIMENTS



Carl-Emil Grøn Christensen
Department of Physics and Astronomy, Aarhus
University

Supervisor:
Gorm Bruun Andresen
Department of Engineering, Aarhus University

June 2016

Abstract

Contents

1	Introduction	1
2	Theory	3
2.1	Basic Rocket Science	3
2.2	Hybrid Rocket Engine	5
2.2.1	Injection	6
2.2.2	Combustion Chamber	7
2.2.3	Throat	11
2.2.4	Nozzle	12
2.3	Heat Capacity	13
2.4	Isentropic Flow	14
3	Simulation	17
3.1	Implementation	17
3.2	Results	19
4	Rocket Tests	22
4.1	Equipment	22
4.2	Experimental Procedure	23
4.3	Results	25
5	Discussion	27
6	Conclusion	29
7	Future Prospects	30
A	News articles	32
B	Rocket Logbook	34
B.1	Day 1	34

B.2	Day 2	34
B.3	Firing Procedure	36
Bibliography		38

1

Introduction

It's not rocket science.

The following report contains simulations and observations of the hybrid rocket MEOWTH II (**M**echanical **E**ngineering **O**bservational **W**ingless **T**utoring **H**ybrid rocket) created by *Team Rocket* [1] at Navitas, Aarhus University. The first rocket was built in 2014 by a previous group of students, but has since been passed along to other students, with the intent of teaching the basics of rocket science.

During the previous MEOWTH's tests, a large pressure spike during the startup phase has been observed. This can be seen in the old video here: bit.ly/1SYp1Ug in the timespan of seconds 5-7. From the video, it appears that just as the rocket exhaust reaches supersonic speeds, *something* explodes, extinguishing the flame. We know it happens before the rocket goes supersonic due to the lack of shock diamonds prior to the event [2].

This bachelor thesis attempts to simulate the rocket's startup condition in order to explain and understand the event. My advisor, Gorm Bruun Andresen, proposed a hypothesis that the pressure spike occurs at the point where mass-flow is choked in the throat. As the flow is sub-sonic, the amount of matter exiting through the nozzle is gradually increasing. When the flow goes sonic or beyond, it is suddenly capped. This abrupt change in physical properties may be able to explain this event, and the following contains the theories and thoughts that went into simulating the rocket engine's startup.

1. Introduction

In order to create a safer rocket with more measurement options, MEOWTH II was built. Gorm Bruun Andresen, Alex Nørgaard, a fellow student, and I personally assembled the rocket. The rocket can be seen on the frontpage and on figure 2.2, and each section contains at least four possible points measurements for various instruments.

The purpose of these simulations are ultimately to improve the rocket and rid it of large pressure variations. To see improvements, it is necessary to measure how the rocket behaves under different conditions. Therefore, setup and calibration of various measurement equipment is essential in order to retrieve excellent data. This is also covered in this report, as the experimental part is of equal importance. Measuring the rocket chamber's temperature is of great inconvenience, as the several thousands of kelvin are too much for even the strongest of thermocouples [3]. This issue and its solution is discussed thoroughly in the sections below.

All measurements and tests could not have been carried out if not for the test facilities provided by Peter Madsen of Raketmadsen's spcelaboratory. MEOWTH II's tests were carried out on the 3rd to the 4th of May, 2016 in Copenhagen.

The entire project is publicly available on https://github.com/carlegroen/bachelors_degree, where all work files, data and various notes can be found.

2

Theory

Understanding the theory behind the rocket's flow requires a basic knowledge of rockets. Therefore, the first theoretical segment concerns basic rocketry, followed by a more advanced segment of nozzle theory.

2.1 Basic Rocket Science

A rocket engine consists of a few fundamental elements. There exists two types of rocket engines, as seen in figure 2.1. A rocket engine is a type of jet engine that, in contrast to duct jets, carry their own rocket propellant. Jet engines as seen in aeroplanes are usually situated with a duct, confining the air flow. Rocket engines on the other hand carry a supply of oxygen and rocket propellant, which allows them to function even in vacuum.

Rocket engines work by obtaining thrust in accordance with Newton's third law. The internal combustion chamber accelerates fluids through a propelling nozzle to high speeds. The fluid is most often a gas created from mixing fuel and oxidizing components in the combustion chamber. The exhaust is accelerated to supersonic speeds by expansion in the nozzle, which forces the engine in the opposite direction.

Most rockets used today are liquid rockets which store their propellant and oxidizing component in separate tanks. The liquid fuel is then forced into the combustion chamber for consumption.

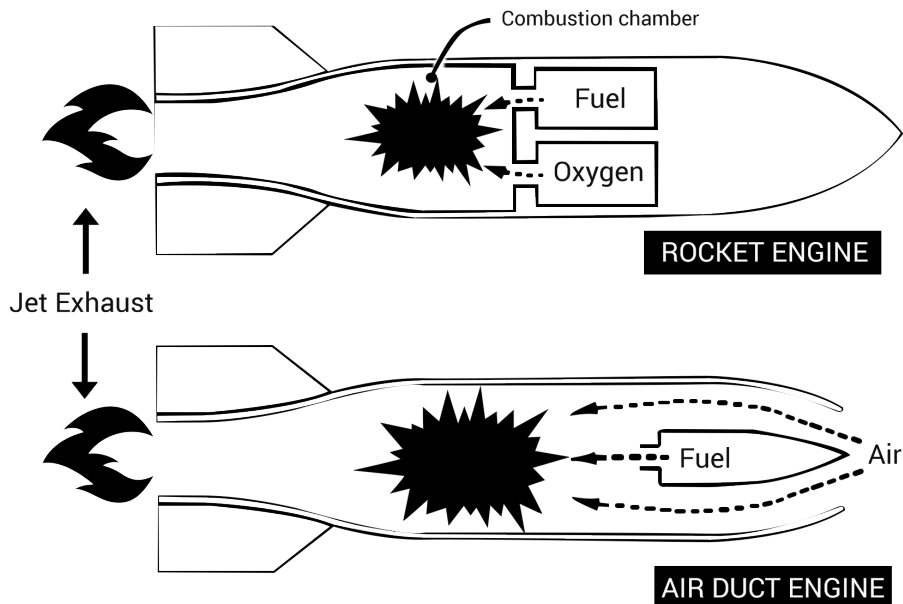


Figure 2.1: Schematic difference of the two types of jet engines: Rocket engines and air duct engines.

Solid-fuel rockets contain propellant prepared with a fixed fuel and oxidizing component. The fuel is called 'grain', and the storage compartment for the grain is the combustion chamber. A hybrid rocket is the mixture between the two. Most often, hybrid rockets contain a solid fuel, or 'grain' and liquid or gaseous oxygen, thus earning the name hybrid engine. Variations of this engine type do exist, but this configuration is the most often used [2]. Solid oxidizers are uncommon as they are problematic and have worse performance than liquid oxidizers.

Liquid and hybrid engines both use injectors to disperse oxygen and propellant into the combustion chamber. For a hybrid engines, this means spreading oxygen to the grains surface to allow combustion.

Hybrid rockets are inherently safer than its two counterparts, and accidents are less volatile as accidental fuel mixing is a non-issue.¹ The oxidizer and fuel are almost always contained in separate chambers, which also reduces the mechanical complexity of the rocket in comparison to liquid rockets.

¹Assuming you can control the oxidizer inlet valve.

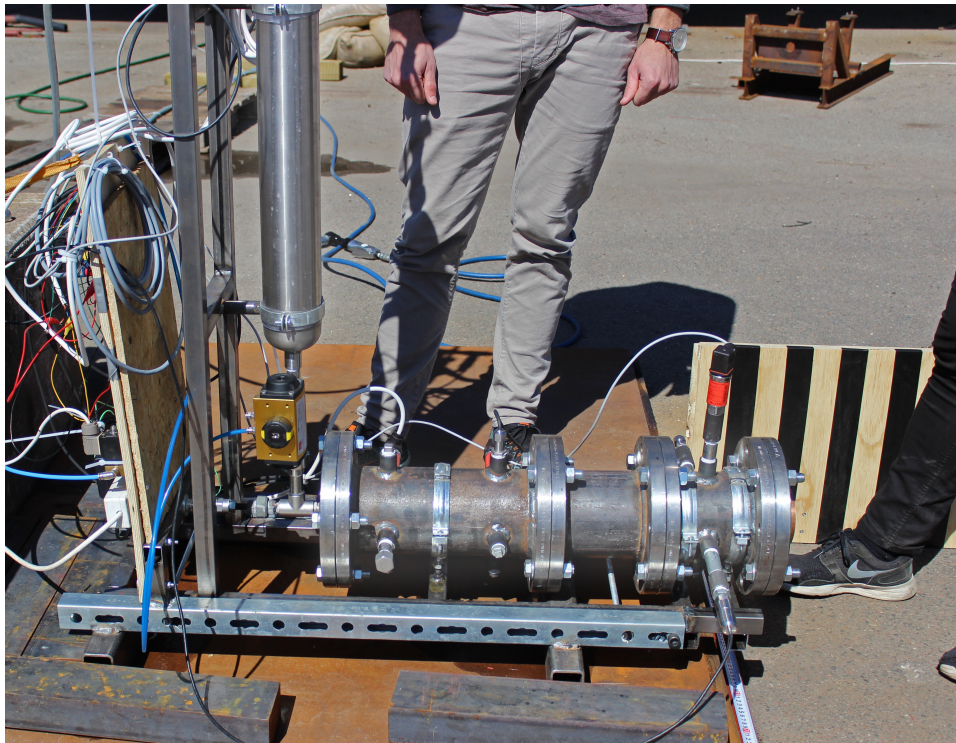


Figure 2.2: The hybrid rocket built at Navitas in Aarhus for educational purposes.

2.2 Hybrid Rocket Engine

The hybrid rocket engine consists of three parts: The combustion chamber, the converging into a throat, and diverging section after called the nozzle. A rocket's effectivity is highly dependent on the shape, size and ratios between these three segments. Accordingly, it is imperative to study these parts of the rocket's design.

The rocket in question is seen in figure 2.2 which is divided into a tank, three chambers and a nozzle. A schematic setup can be seen in figure 2.3.

From the left: The tall tank marked with a 1 contains the oxidizing agent, which is injected into the first part of the rocket. The oxidizing agent used is hydrogen peroxide in an 80% concentration. Point 2 marks the place where the injecting nozzle is placed, which determines the rocket's mass flow rate. The longest part of the rocket, as seen on figure 2.3 marked with 3, contains potassium permanganate engulfed in a flame retardant foam. The mixing of potassium permanganate and hydrogen peroxide rapidly creates

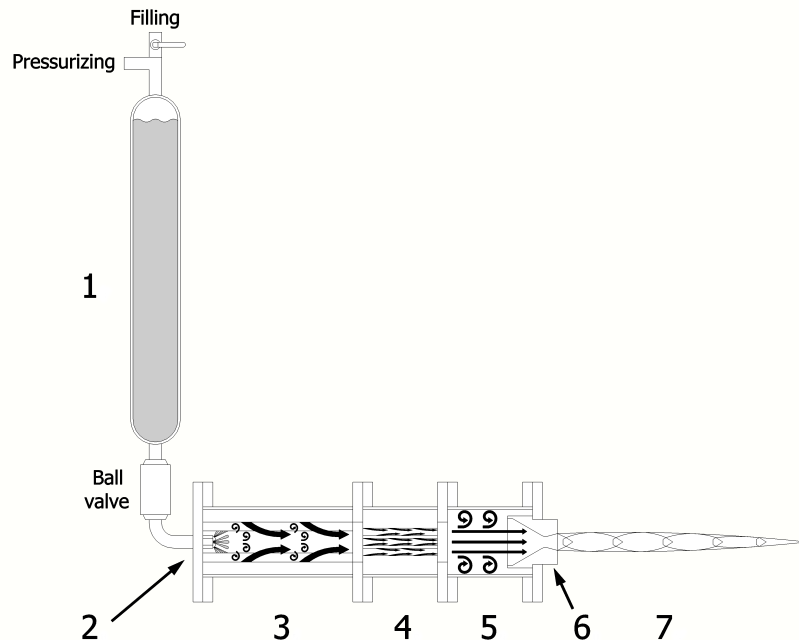


Figure 2.3: Cross section of the rocket.

large amounts of oxygen, which is forced through the rocket's second part: the grain chamber, marked with numer 4. The rocket's main fuel is plain Medium-Density Fiberboard (MDF), which resides here. The energy released during decomposition heats the wooden MDF grain, until temperatures reach MDF's autoignition point of 492K at atmospheric oxygen levels [4]. Around this point the fuel combusts, and the exhaust exits through the nozzle 6 after it has passed the mixing chamber 5.

All calculations and considerations made in the report is in regard to this particular rocket. The following subsections each elaborate individual segment of the rocket, with the purpose of providing the necessary background knowledge to understand the ignition simulations and results. The explanation is given step by step, starting with injection and ending with exhaustion.

2.2.1 Injection

To initiate combustion in the hybrid engine, an oxidizer is injected into the combustion chamber. The rocket in question creates its oxidizer by mixing an oxidizing agent with potassium permanganate. The agent is contained in a pressurized tank containing an 80%

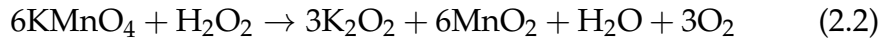
2.2. Hybrid Rocket Engine

H_2O_2 rich mixture with the remainder being H_2O . The oxidizing agent is assumed to be injected at a constant rate of:

$$\dot{m}_{\text{injection}} = 0.246 \text{ kg s}^{-1}. \quad (2.1)$$

in accordance to data collected at the recent launch [5].

The oxidizing agent is injected into the first chamber where decomposition into O_2 is aided by potassium permanganate. The hydrogen-peroxide (H_2O_2) decomposes into dioxygen (O_2) as it reacts with the potassium permanganate (KMnO_4), which is encased in a flame retardant foam. The balanced chemical redox reaction is as follows:



The specific enthalpy released during decomposition is:

$$\Delta h_{\text{decomposition}} = \frac{\Delta H_{\text{H}_2\text{O}_2}}{M_{\text{H}_2\text{O}_2}} \quad (2.3)$$

Where ΔH is the change in enthalpy. The energy released heats the grain's surface to autoignition temperatures of approximately 220°C in this extremely oxygen-rich environment. The increased temperature increases the pressure, in accordance to the ideal-gas law:

$$PV = nRT \quad (2.4)$$

Which is assumed to be valid as the gas is approximately stagnant in the mixing chamber [6]. The ideal gas law is crucial in our description of the rocket. Describing the rocket's upstart phase requires coupling the changes in temperature T , pressure P and amount of substance n . During injection and decomposition, combustion occurs simultaneously.

2.2.2 Combustion Chamber

The combustion chamber contains two important theoretical aspects. First, the propellant grain has significant effects on the rocket's thrust over time. Secondly, the theoretical description of the rocket's combustion allows us to estimate different working parameters, and deciding the rocket nozzle's size and area ratios.

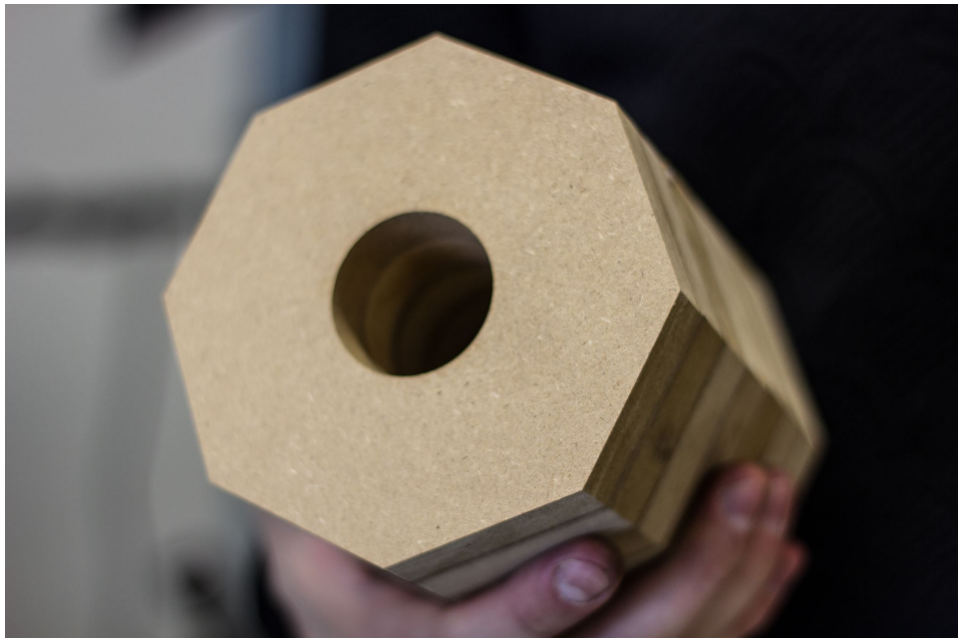


Figure 2.4: Example of MDF grain with a single combustion-hole. This will have a uniformly increasing regression-rate, as the burning area increases evenly.

Propellant Grain

The combustion chamber consists of an approximate 3 liter cavity which is filled with the grain. The actual volume in a hybrid rocket depends strongly on the initial condition of the grain and the fuel's combustion rate. Holes have to be carved in the grain to allow oxygen to reach the grain's surface, and transport exhaust towards the throat. The combustion rate is largely determined by the exposed surface area of the grain, and the flux of the oxidizer. The surface gradually expands as the outer regions are burned away, thus changing the rocket's effective thrust over time [7]. The propellant's increase in burning area during ignition is assumed to be negligible, compared to the rapid increases in pressure and temperature.

The shapes and sizes of the holes in the grain has a large impact on the initial ignition and thrust ratios [8]. An example of a single hole configuration can be seen in figure 2.4, and more examples can be found on http://www.nakka-rocketry.net/th_grain.html, along with a general performance description. Depending on the surface areas and designs, the different grain's regression rate varies greatly over time. The regression rate will be proportional to the

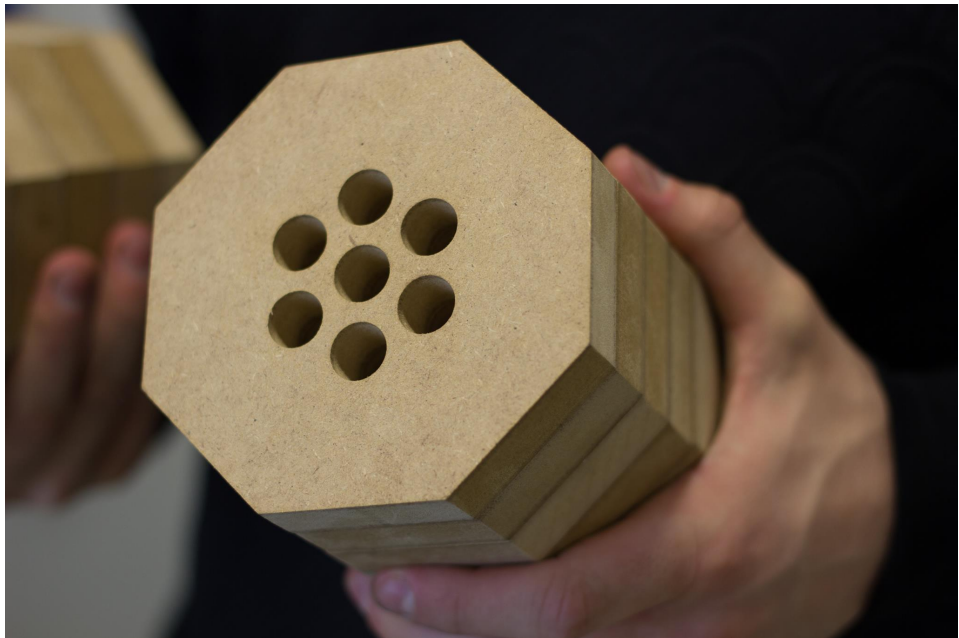


Figure 2.5: The wagon-wheel design used in all rocket tests concluded in this report. The large surface area allows combustion to be more efficient.

thrust, unless oxygen is the limiting factor. The generated thrust is directly proportional to the instantaneous burning area, and as this area increases, so does the thrust.

An alternative explanation to the pressure spike could therefore be a very fast increase in regression area. The grain's specifications from the previous tests are not mentioned, but a wagon-wheel design as seen in figure 2.5 with several holes could allow ignition in single canals before all of them. This could allow hot pyrolytic fuel and oxygen to accumulate, causing an eventual explosion. The large surface area of the wagon-wheel design allows for cleaner, more efficient combustion, and it is therefore the preferred setup for our experiments [8].

Autoignition

There are two types of ignition: Autoignition and piloted ignition [9]. Piloted ignition is the process of flame propagation in a premixed fuel system, such as lighting a candle or starting a petrol engine. This is the usual way of igniting every day systems, however, MEOWTH uses the other type: Autoignition.

Autoignition occurs without a spark of flame present. The fuel must have a certain concentration and temperature, before spontaneously igniting. This temperature is lowered by rising oxygen concentration and pressure, which complicates setting a specific point of time of ignition [10]. According to the MDF's datasheet [4], autoignition occurs around 220 °C to 250 °C. This minimum temperature tells us when spontaneous combustion takes place, the question is then how quickly after reaching this temperature does the material ignite?

Autoignition time t_{auto} for thick materials (thicker than 2 mm) is given by:

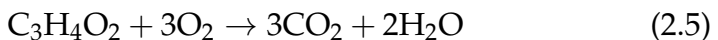
$$t_{\text{auto}} = C(k\rho c) \left[\frac{T_{\text{auto}} - T_{\text{initial}}}{\phi} \right]^2$$

where k is the thermal conductivity of the material, C is a constant depending on the heat flux, but roughly equivalent to 0.785 assuming no heat loss [9]. T_{auto} is the autoignition temperature and T_{initial} is the starting temperature, and ϕ is the heat flux.

Back-of-the-envelope calculations show that the autoignition time is on the order of magnitude 10^{-5} s, which is way faster than anything we should be able to measure. The temperature and pressure rise far too quickly for this to have an obvious effect on the ignition. It is thus assumed to be far too small to have any real influence, compared to the autoignition temperature.

Combustion

As temperatures reach the MDF's autoignition point, and oxygen levels increase, combustion starts taking place. The combustion reaction can be described chemically by the formula:



Energy released in this reaction heats up the chamber's fluids towards a design temperature of 2498 K. Assuming a *closed* chamber, the rise in temperature and amount of substance yields a rapid increase in pressure over time. This is not a desired property, as that would eventually lead to engine destruction. The accumulated decomposed and combusted material leaves through the rocket's throat, which allows the rocket to reach pressure-equilibrium. The throat's area is essential to the rocket's pressure and thus stability, hence the advance to the throat.

2.2.3 Throat

The throat begins at the end of the combustion chamber, at the opposite side of where injection occurs. The throat is characterized by the convergence of the rocket chamber into a small passage called the throat, followed by a diverging section: The nozzle. The throat can be seen schematically on figure 2.6. The throat's cross-sectional area is what determines the maximum flow rate, as the speed of sound restricts the flow of matter. In order to calculate the amount of matter contained in the chamber, it is crucial to know how much is flowing out. Due to conservation of mass, the flow rate \dot{m}_t must be proportional to the density of the material, the velocity and the throat's area according to [11]:

$$\dot{m}_t = \rho_t \cdot v_t \cdot A_e \quad (2.6)$$

The velocity v_t is thus roughly proportional to the mass flow as the area and density are approximately constant in this case. Hence, as the matter approaches the speed of sound, the flow rate out of the rocket stagnates. This is called mass flow choking, which must be at a maximum when the velocity is equal to the speed of sound. This condition is satisfied when the mach number $M = 1$, or given by the pressure relationship from [12]:

$$\frac{P_e}{P_0} \leq \left(\frac{2}{\gamma + 1} \right)^{\frac{\gamma}{\gamma - 1}} \approx 0.56 \quad (2.7)$$

where P_e is the exit pressure (equal to ambient), P_0 is the chamber's pressure and γ is the isentropic expansion factor. As long as this relationship is not fulfilled, the mass-flow obeys equation 2.6

For an ideal compressible gas, this becomes:

$$\dot{m}_t = \frac{A_t P_c}{\sqrt{T_t}} \sqrt{\frac{\gamma}{R}} \left(\frac{\gamma + 1}{2} \right)^{-\frac{\gamma+1}{2(\gamma-1)}} \quad (2.8)$$

Where P_c is the pressure in the combustion chamber, T_t is the temperature in the throat, γ is the specific heat ratio and R is the gas constant [11]. Three outcomes are possible:

$\dot{m}_t < \dot{m}_{in}$, less mass is coming out than is flowing "into" the rocket.

$\dot{m}_t = \dot{m}_{in}$, mass outflow equilibrium.

$\dot{m}_t > \dot{m}_{in}$, more mass is flowing out than is being created.

The first outcome would yield increasing pressure until the rocket has burned all of its fuel, or it explodes. The second option is what we know as a safe and steady rocket, assuming the designed mass flow equilibrium is within the rocket's boundaries. The final outcome will yield a slow decrease in pressure over time, until the rocket has been exhausted for material inside and combustion ceases.

FIXme Note: Passer det med masse?

In order to describe the initial pressure spike it is necessary to not assume any of these conditions. The abrupt change from the first to the second condition was initially hypothesized to cause the spike in pressure. Therefore, simulating the mass flow out of the rocket is essential to our understanding of the phenomenon. This does however require knowledge of several key parameters within the rocket, which are difficult to calculate, unless some things are assumed, such as conservation of entropy. However, in order to combine this knowledge, we first have to look at the final piece of theory.

2.2.4 Nozzle

The rocket nozzle's primary function is to channel the combusted propellant out of the rocket and accelerate it. The optimal nozzle maximizes the velocity of the exhaust, preferably to supersonic values. The most well-known nozzle is a convergent-divergent nozzle called a de Laval Nozzle, which performs all of these things through simple geometry. Such a nozzle can be seen on figure 2.6, where the combustion chamber is to the left, and the exhaust is to the right. The flow's velocity increases from green to red in the direction of the flow. An important part of maximizing the nozzle's performance is ensuring that the flow stays isentropic. Isentropic flow requires that the flow is frictionless and adiabatic, which ensures entropy is conserved. Isentropic flow is considered to *only* be dependent on the cross-sectional area of the nozzle that the fluid moves through [14]. This allows calculation of any variable in any place, given some initial conditions.

As the fluid is pushed through the throat it is highly pressurized. The nozzle is in contact with the surroundings, which acts as a reservoir of low-pressure gas between atmospheric pressure (101.3 kPa)

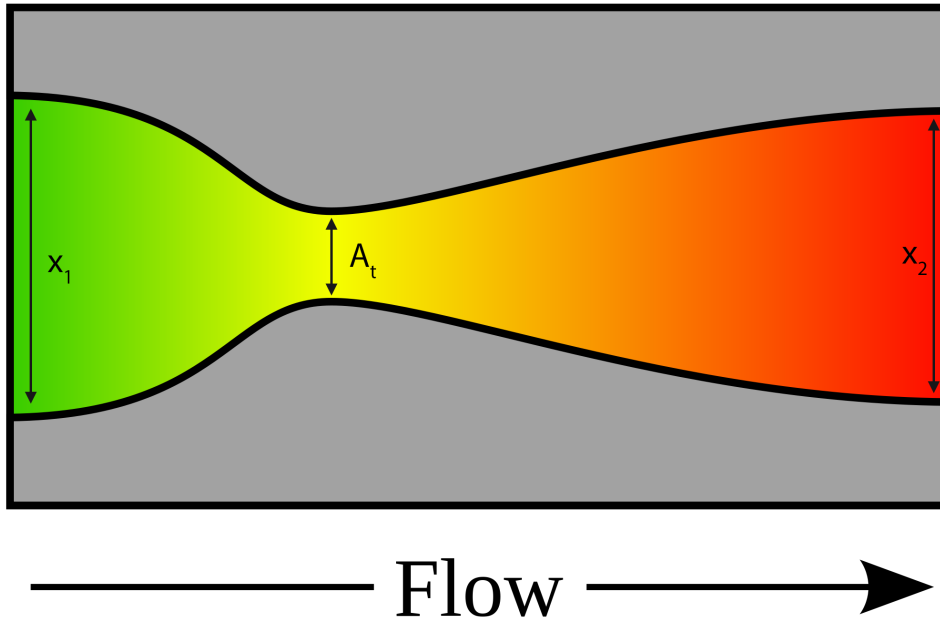


Figure 2.6: Schematic of a de Laval nozzle, where the green area is equivalent to the mixing chamber, and the red area is the nozzle's exit. x_1 and x_2 are points where one could use isentropic relations to decide the rocket's conditions. Picture taken from [13].

and no pressure (in space!), depending on the rocket's whereabouts. The expansion of course depends on the surrounding pressure, but in general, the plume can be over- and under-expanded and ambient. Ambient is the preferred expansion of the plume, where the exhaust gas is in pressure equilibrium with the surrounding air. If the exhaust has the same pressure as the surroundings, the gas is optimally expanded, and provides the maximum amount of thrust to the rocket [15].

2.3 Heat Capacity

The rocket's internal energy can be approximated as a closed system, which changes by adding heat through combustion or decomposition. Heat capacity is a measurable physical quantity, which is proportional to the ratio of heat added to the system, to the resulting change in temperature. The heat capacity ratio is denoted by γ (or κ

by mechanical engineers), and it is given by the equation:

$$\gamma = \frac{C_p}{C_V} \quad (2.9)$$

γ being the ratio between C_p , which is the heat capacity at constant pressure, and C_V which is the heat capacity at constant volume. γ is also known as the isentropic expansion factor, which is essential in the next section [16].

The heat capacity ratio for various gases changes with temperature, albeit very little [17]. In order to simplify the calculations, the heat capacity ratio for the rocket's fluids is assumed to be constant at $\gamma = 1.2$. This is a rather crude simplification, as the heat capacity ratio can change with upwards ± 0.1 in the temperature and pressure ranges we are working. Complications with the simulation software EES did not allow a continuous recalculation in every iteration, however.

2.4 Isentropic Flow

In order to effectively describe the rocket's behavior, we have to assume a few things:

1. Entropy is conserved.
2. Decomposition and combustion products obey the perfect gas law.
3. All chemical reactions are adiabatic: No heat is lost to the surroundings.
4. The fluid velocity inside the chamber is approximately zero, allowing us to assume stagnated pressure. The velocity is *not* assumed to be zero when entering the throat and nozzle, however.

The assumption of isentropic flow stems from the idea that the process is reversible. The fluid will, after moving through the nozzle, have the same original values. The second law of thermodynamics states that reversible flow maintains entropy, and this allows us to calculate almost any value related to the rocket's flow. It is therefore an essential piece to the project [14].

If supersonic flow is not achieved by gradual means, isentropic flow is not a valid assumption. If shock waves occur abruptly, isentropic

2.4. Isentropic Flow

flow is not a valid assumption. Hence, exit values are simulated before any normal or oblique shock relations occur [18].

The simulation is based on four valuable equations: The conservation of energy, the continuity equation, the momentum equation and equation of state.

Conservation of energy requires that for adiabatic flow, between two any points x_1 and x_2 , as seen in figure 2.6:

$$h_1 - h_2 = \frac{1}{2} (v_2^2 - v_1^2) = C_p(T_1 - T_2) \quad (2.10)$$

where h again is the enthalpy of the fluid, v is the flow velocity and C_p is the heat capacity, T is the fluid's temperature. From the continuity equation, we can find a pseudo-steady state from looking at the stagnation temperature in the chamber. Setting $v_2 = 0$ yields the stagnation temperature:

$$T_0 = T + \frac{v^2}{2C_p} \quad (2.11)$$

This yields several key relationships between stagnation properties for pressure, density and temperature according to [19]:

$$\frac{T_0}{T} = \left(\frac{P_0}{P} \right)^{\frac{\gamma-1}{\gamma}} = \left(\frac{\rho_0}{\rho} \right)^{\gamma-1} \quad (2.12)$$

Using this, we can find the temperature at the exit:

$$T_e = T_0 \left(\frac{P_e}{P_0} \right)^{1-\frac{1}{\gamma}} \quad (2.13)$$

As P_e is the exit pressure, which is equivalent to the ambient pressure. The exit temperature allows us to calculate the density of the exiting fluid ρ_e :

$$P_e = \rho_e R T_e \Rightarrow \rho_e = \frac{P_e}{R T_e} \quad (2.14)$$

Bernoulli's equation provides us with the exit velocity v_e :

$$v_e = \sqrt{2 \frac{P_0 - P_e}{\rho_e}} = \sqrt{2 \frac{P_0 - P_e}{\frac{P_e}{R T_e}}} \quad (2.15)$$

$$= \sqrt{2 \frac{(P_0 - P_e) R T_e}{P_e}} \quad (2.16)$$

Exit velocity and density yields the mass outflow per second:

$$\dot{m}_{\text{out}} = A_e \cdot v_e \cdot \rho_e \quad (2.17)$$

and knowing how much matter is flowing "into" the rocket (see injection and combustion chamber sections) yields the total enthalpy contained in the rocket at all times. Therefore, we can now approximate the temperature in the rocket's chamber, knowing the different material's abundances. In general, the internal energy and temperature for a reversible process at constant volume is given from [6]:

$$dU = C_V dT \quad (2.18)$$

where dU is the change internal energy, C_V is the specific heat capacity at constant volume and ΔT is the change in temperature. Enthalpy in a homogenous system is given by $H = U + PV$ [20], where P is the pressure and V is the volume, thus yielding the temperature:

$$U = H - PV = C_V T \quad (2.19)$$

$$T = \frac{H - PV}{C_V} \quad (2.20)$$

As the temperature rises for several different molecules at once, this becomes more complicated. To calculate this, a commercial software called *EES* is used. The general gist of the solution is that

$$T = \frac{H - PV}{C_{V,1} + C_{V,2} + \dots + C_{V_n}} \quad (2.21)$$

where $C_{V,1} \rightarrow C_{V_n}$ is the specific heat capacity for all molecules in the mixture. A full description can be found in [21].

3

Simulation

Using the previous theory, simulating the rocket's ignition phase can be done using only a fairly small sample of data. Molar masses, gas constants and the like are all table constants. Given ambient pressure P_0 , temperature T_0 and chamber volume V_{chamber} , initial conditions can be calculated. As the rocket takes off, using the mass flow \dot{m} and fraction of oxygen being consumed in combustion f , we can compute the rocket's performance at all times assuming isentropic flow. The inner pressure and temperature can be found by calculating the flow into and out of the rocket, as well as the energy released in the various chemical reactions.

3.1 Implementation

The rocket engine's ignition algorithm is based on the previous assumptions. Figure 3.1 shows a flowchart of the ignition algorithm. The implemented algorithm is divided into four parts, which determine the rocket's performance at various stages. The first stage is the rocket's pre-launch conditions, eg. amount of substance n , pressure P and temperature T . The second stage is injection of oxidizer into the pre-combustion (or decomposition) chamber. The amount of injected oxidizer is equivalent to the injection nozzle's flow per time step Δt in every iteration. This is followed by recalculating the rocket's conditions. After the initial matter has been injected, decomposition starts. This is the third stage of the algorithm. Post

3.1. Implementation

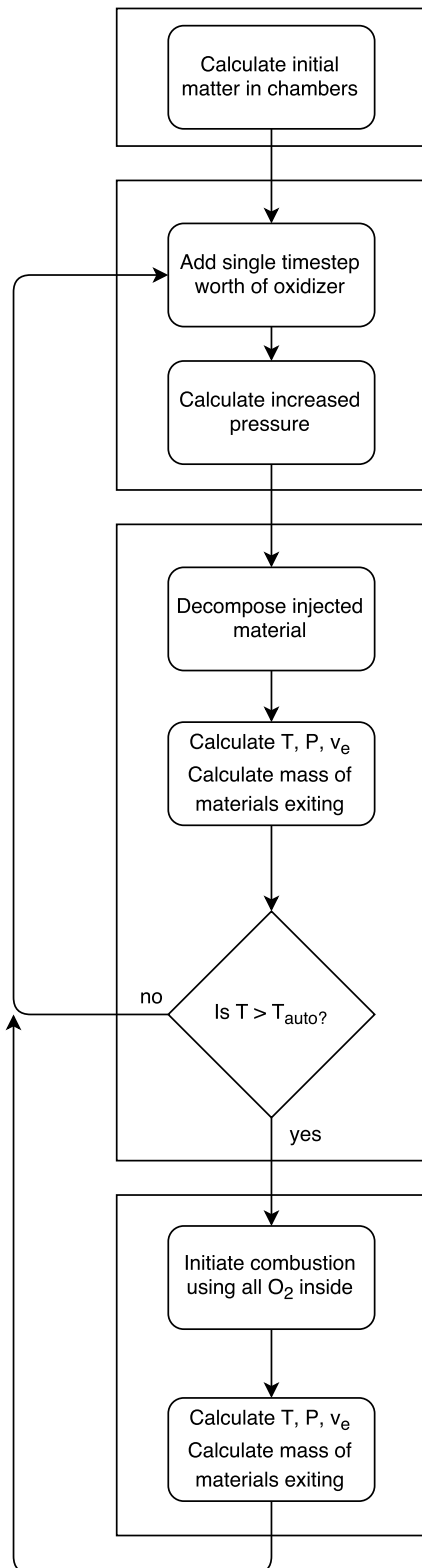


Figure 3.1: Scheme showing the implementation of the rocket's ignition algorithm.

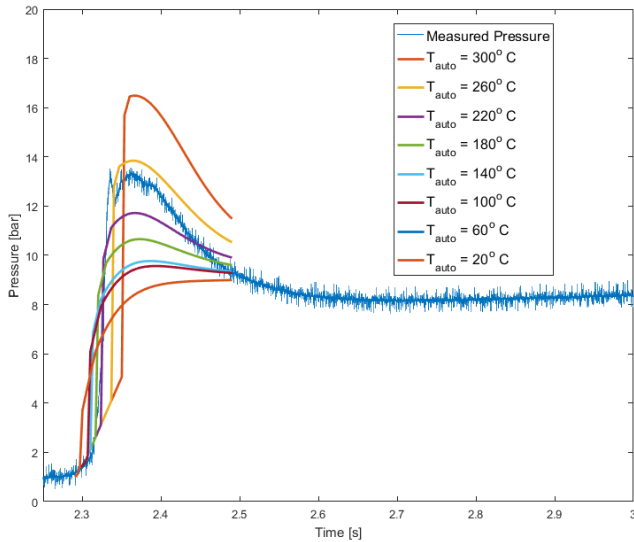


Figure 3.2: Pressure over time for different autoignition temperatures T_{auto} . The highest peak is given by the highest autoignition temperature.

decomposition, the temperature, pressure, exit velocity v_e and exit mass can be found. The temperature is compared to the autoignition temperature T_{auto} : If higher, combustion of material still contained inside the rocket starts. Otherwise, more oxidizer is injected and decomposed until the energy released during decomposition heats the interior to autoignition temperatures. The final stage occurs when temperatures are large enough to allow combustion. Combustion expends *all* the available oxygen inside the rocket during every iteration. This means, that if $T_{\text{auto}} \approx T_{\text{amb}}$, combustion occurs instantaneously, using only the oxygen released by the first time step's oxidizer. If, however, $T_{\text{auto}} > T_{\text{amb}}$ (as it is in our case), combustion occurs a certain time later, allowing oxygen to accumulate inside the chamber.

3.2 Results

The simulation shows promising results in the description of the hybrid engine's pressure spikes. As it appears from figure 3.2, the higher the autoignition temperature the higher the peak pressure is. Thereto, the higher the peak, the later combustion takes place. This

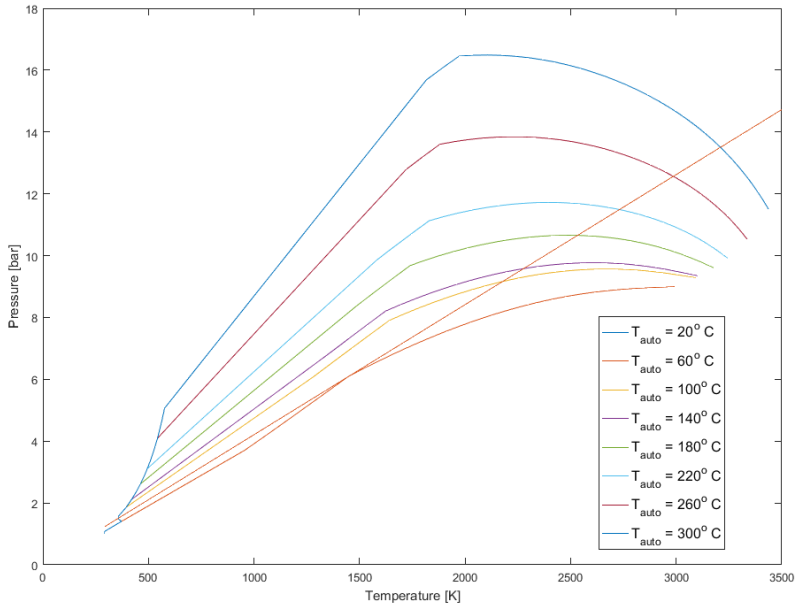


Figure 3.3: Pressure per temperature for different autoignition temperatures T_{auto} .

is to be expected, as a higher autoignition point allows more oxygen to accumulate in the chamber which of course takes more time. All of the simulations tend toward a steady-state at the end, where they would eventually meet at the design-pressure. The yellow, low auto-ignition point of 60 °C steadily and cleanly tend toward the design-pressure, as would be preferred for the hybrid rocket. The steady increase ensures no rapid combustion happens, and transitions between the ignition states flow without problem. This result proposes the hypothesis, that a reduction of the autoignition temperature, or the presence of a pilot flame might be able to extinguish the unwanted spiking behavior.

In figure 3.3 we see the pressure plotted against temperature in the simulation, with a theoretical fit of the rocket's design values. After initial spiking, the pressure drops as the temperature increases up to very large values of almost 3500 K. The pressure should stabilize steadily towards the end, but all simulations show a trend of pressure dropping with increasing pressure. However, the rocket is designed to work at a temperature of 2500 K, and the pressure values around this area varies between 8.8 bar and 16.2 bar – somewhat

3.2. Results

within the design pressure of 10 bar.

4

Rocket Tests

MEOWTH II was tested at Peter Madsen's space laboratory in Copenhagen, on the 3rd to the 4th of May 2016 by Team Rocket of Navitas. The whole ordeal has spawned several articles, which the interested reader can find in appendix A. A complete logbook along with a firing procedure can be found in appendix B.

The test setup can be seen in figure 2.2, and the first burn can be seen on the front page. The test stand consists of a metal fixture that holds the rocket in a vertical position, with the hydrogen–peroxide tank upright. The metal fixture keeps the rocket from moving under tests. Sandbags are placed on top in order to stop fast-moving shrapnel, in case of a complete engine destruction. Further safety instructions can also be found in appendix B.

The purpose of the experiments was to measure the variations in pressure throughout the rocket. The following will be an analysis of the data collected, along with a brief description of the sensors involved. A group consisting of three students also took video footage of the tests in order to analyze the rocket's shock diamonds, this will not be treated here, however.

4.1 Equipment

Eight pressure sensors were mounted on the rocket, ranging over three measurement frequencies: 250 Hz, 2000 Hz and 20 000 Hz. All were measured at 20 000 Hz, which means the slower sensors are



Figure 4.1: Foam permeated with KMnO_4 dust inserted into the decomposition chamber, inside a tube of MDF, in order to avoid accumulation of liquid H_2O_2

oversampled. One of each sensor was placed in both the rocket's mixing chamber and decomposition chamber. The two remaining sensors, a slow and a fast, were mounted by the hydrogen-peroxide tank. The measurement equipment was connected to a DAQ system from National Instruments, which in turn was connected to the data-logging software LabVIEW on a nearby slave unit. The slave unit was remotely controlled by a computer inside the safety-submarine, which allowed ignition and data-logging nearby the test site without being in danger.

Two manometers were placed before and after the pressurization valve, in order to manually check the tank's pressure before ignition. A more thorough discussion of project improvements can be found in chapter 7.

4.2 Experimental Procedure

MEOWTH II was built specifically with the intent of being fast to rearm. The large flanges allows quick unbolting, and the hydrogen-peroxide tank has a quick-fill valve. The only swappable objects



Figure 4.2: Wagon-wheel shaped grain as seen in figure 2.5 after a test. Notice the wagon-wheel pattern has been burnt through, and instead a "flower"-pattern is present. Experimentally this can be seen as a small drop in pressure as seen in the results.

which changes the combustion rate is the decomposition nozzle and the fuel–grain. The tank’s pressurization changed throughout the experiments, which greatly influences the flow–rate of hydrogen–peroxide. An analysis of the tank’s pressure’s influence on flow–rate has not been executed, however, that could be a subject for a future project. The wagon–wheel fuel grain design (see figure 2.5) was kept throughout the experiments, which makes the decomposition nozzle the only variable in the experiments.

Apart from changing larger parts of the experimental setup, reloading procedure requires swapping the rocket’s interior. In figure 4.1, the decomposition chamber is visible with its inner MDF–shell casing, filled with KMnO₄–permeated foam. The inner casing prevents liquid puddles from not building up and causing trouble, in the form of instant vapourization into large quantities of gas.

Swapping the wagon-wheel grain with an identical copy after every test is essential to receive consistent results, as it is worn greatly during combustion. As seen in figure 4.2, the grain's inner walls are burnt through about two-thirds through every test. This greatly influences the grain's regression-rate, making new- and old-grain experiments vastly different.

Preliminary tests were done with water, as to check the newly made decomposition nozzle. Testing with water also showed leaks, making it easier to tighten and seal the piping before loading the toxic high-concentration hydrogen-peroxide. After preliminary tests, four tests were concluded and will be discussed below.

4.3 Results

All tests used 1.3 L of hydrogen-peroxide, making the injection rate easy to calculate assuming linear flow. In figure 4.3 the resulting pressure over time graphs are seen. As seen in the figure, higher tank pressure appears to influence the spike's height. It is questionable whether or not the spike in test three and four are representative, as data on the top appears "flattened", as if the pressure went further than the set measurement range for a brief amount of time. After the spike, the graphs flatten out and slowly decrease until they all drop slightly in pressure. This drop is most likely due to the grain's design. The wagon-wheel design seen in figure 2.5 has a large surface area for combustion. After burning for some time the grain's wall regress far enough to create a larger cavity, but drop in overall surface area as the walls collapses to a flower-pattern as seen in figure 4.2. As the walls are burnt through, the surface area decreases and in turn, so does the regression-rate and combustion rate. This reduces the chamber pressure by approximately 20%.

As the rocket is ignited noise starts to arise. This gives a clear indicator of when rocket ignition happens, but at the cost of accuracy. The noise was an unwanted feature, which stems from an accidental ground-loop in the test-setup. The rocket burns are all zeroed around the noise which shows when ignition starts after opening the ball-valve.

The first test shows a significantly slower ignition than the three

4.3. Results

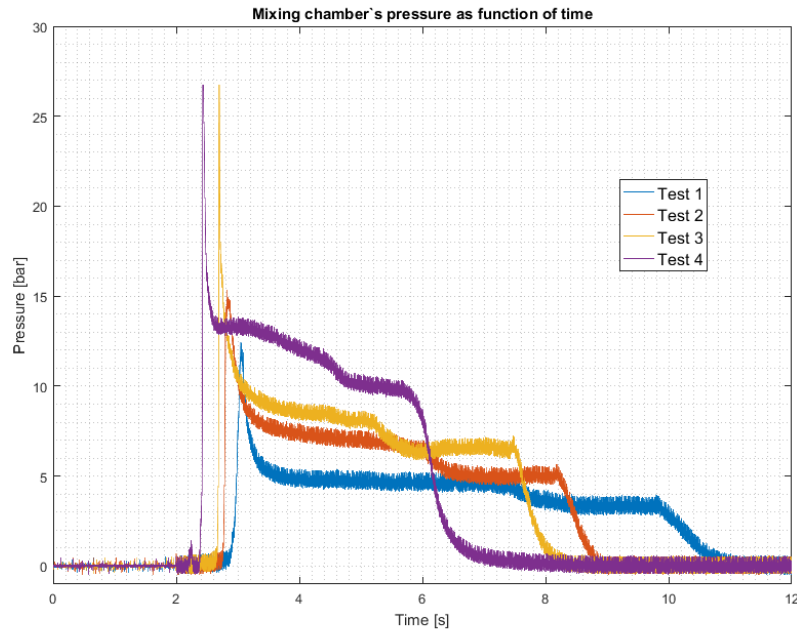


Figure 4.3: Results from the four tests. Test one through four was done with pressures of 24 bar, 24 bar, 31 bar and 31 bar respectively. The last test was done with a larger injector.

others, which is most likely due to the flanges not being tightened correctly, leaking gas out the sides. Test 2 and 3 have almost identical ignition timing, although their tank–pressures differ by 7bar. Their injectors are identical, which makes the change in spike size and timing dependent on the mass flow. It also appears that test 2 and 3 have a duration difference of almost 1 second, which is given only by the change in pressure. The final test have identical tank–pressure to test 3, but with an injector with higher flow–rate. The size of the spikes are seemingly identical, however, upon further inspection it appears that the peaks are flattened due to a too low sample–range. Thus, the peak heights are not exactly representative. Interestingly, the time before ignition happens is shorter with the higher flow–rate injector. It is also quite visible that test 4 concludes much faster than the rest, after only approximately 4 seconds from initial injection, compared to the usual 6 to 8 seconds.

5

Discussion

The following section will discuss the measurements made in chapter 4 and the simulations made in chapter 3. Specifically, the purpose of this paper has been to find a theory as to why the rocket's ignition is troubled by pressure spikes. Comparing simulated situations with real life results may yield a plausible hypothesis.

Figure 3.2 shows a simulation with $\dot{m} = 0.245 \text{ kg s}^{-1}$, which is equivalent to burn 2's flow-rate. The simulation is plotted on top of the second burn, for the purpose of comparing the two results. As it can be seen from the figure, an autoignition-temperature between 220°C to 260°C fits the experimental data quite well. The two simulated curves cover the area where the experimental results lie. The simulation assumes accumulation of oxygen inside the chamber, and with an autoignition temperature of 220°C to 260°C , autoignition instantaneously combusts the hot pyrolyzed oxygen and fuel corresponding to the pressure-spike observed.

Simulating the changes in mass-flow with a steady auto-ignition temperature of 220°C gives figure 5.1. The figure shows, that with sufficiently high mass-flow rate the pressure-spike should go away. However, this comes at the cost of a higher steady-state pressure. This is equivalent what happened in the experiments: Increasing the tank's pressure increases the mass-flow rate, which *should* remove the spike. Withal, the pressure spike is still observed. This questions whether the autoignition temperature is the key; increased flow-rate should yield faster decomposition and temperature increase.

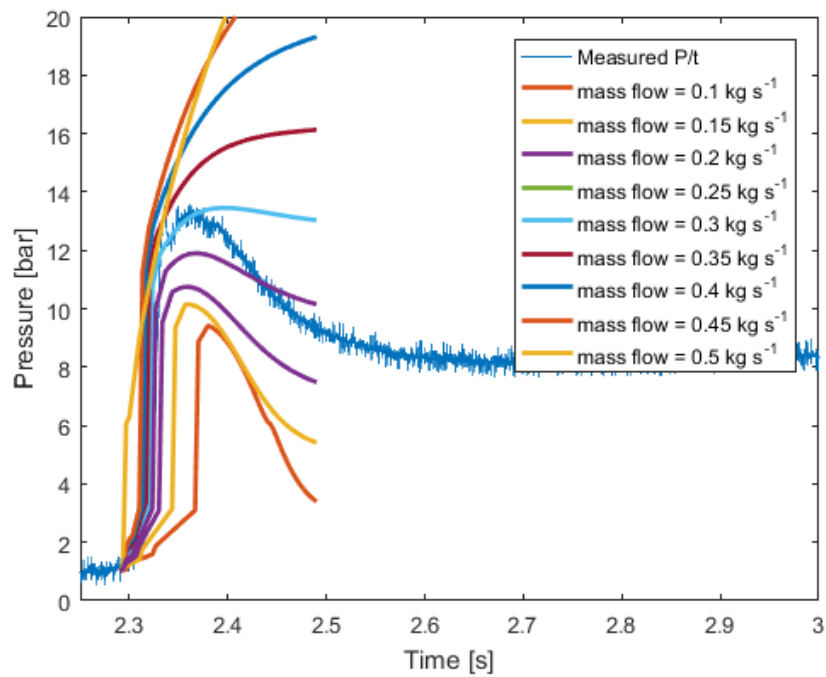


Figure 5.1: Pressure as a function of time for various mass-flow rates. Note that the lowest mass-flow rates are at the bottom, and the highest are at the top.

One could propose that autoignition time is larger than expected or that decomposition happens at a time-scale much larger than the assumed nigh-zero.

6

Conclusion

From my simulation, I propose the hypothesis that the time it takes for the fuel and oxidizer to reach autoignition temperatures is the culprit of the pressure spikes observed at ignition. The proposed hypothesis is that the lower the autoignition temperature, the lower the pressure spike. Therefore, adding a preburner fuel such as ethanol or something with a low autoignition point should reduce this spike greatly. A pilotflame might be the solution to this problem as well, as piloted ignition occurs at lower temperatures, expending the available oxygen faster.

A proposed test experiment could be to add silane (H_4Si), white phosphorous (P) or carbon disulfide (CS_2), all which have very low ($21\text{ }^{\circ}C$, $34\text{ }^{\circ}C$ and $90\text{ }^{\circ}C$) autoignition points. These may work suitably as a self-igniting pilot flame, until the MDF's autoignition point is reached. Alternatively, an "anti-test" can check the hypothesis: Increase the grain's autoignition temperature, in order to see how it behaves in the opposite limit. By increasing the autoignition temperature, a higher pressure-spike should be observed. Furthermore, pre-heating the grain to *just* below its autoignition temperature using electrical heating would allow almost instant combustion as soon as oxygen reaches the heated surface. This should could quite easily be tested and controlled, which makes it a possible project for the next group of rocketeers.

7

Future Prospects

the rocket has room for lots of improvement. The following is a collection of ideas, that work as a to-do list for future rocketeers. It is a mix of rocket-technical improvements, and ideas on how to improve the simulation used in this project.

After initial combustion, the resulting shockwave may move faster than the flame velocity, thus quickly extinguishing the flame before resuming a steady state. This may be an explanation for the small dip in observed pressure around the initial spike seen in the test. Thus, this is someone worthwhile calculating if moving on further with the project. The solution is probably contained in the book *The Principles of Fire Behaviour*, as found in the bibliography [9].

Simulating the change in heat capacity is also essential in order to get a more precise result. Therefore, this is an obvious place to expand on the already established code.

The control computer should be replaced by a microcontroller, such as an arduino or raspberry pi. As of this project, the data bandwidth is too low in either alternative, but it is a viable solution in the near future.

In order to reduce reload time, adding more piping to the christmas tree is necessary, as air leaving the H₂O₂ tank flows back, spilling the H₂O₂ concentration out of the funnel. When a suitable final design is

7. Future Prospects

done, welding the pieces together is a superior alternative to using bolts and nuts. Welding removes any chance hydrogenperoxide leaking, damaging the rocket and measurement equipment.

The rocket's arming and controlpad needs to be set up in a smarter, more convenient way. The ideal setup is to have a single controlbox, that when starts data-collection as soon as the rocket is armed, and notes when it is fired. This would allow everything to be controlled from a single box, with measurements being saved to a raspberry pi situated at the base of the rocket. Data can then instantaneously be read from a secondary computer through cable or wireless connection. As the rocket's final destination is space, continuously improving data-transfer and making the rocket an individual unit is paramount.

Removing additional noise from measurements can easily be done avoiding ground-loops. The ignition controlpad was grounded differently than the other equipment, which introduced another way for electricity to run to ground.

The propellant MDF-grain proved to work very well. However, the glue holding the many pieces together showed to retard the flame-spreading greatly, perhaps impairing the rocket's burn-rate. Every test showed searing of the outside of the grain, except where the glue had penetrated the wood. In future optimizations, this may be cause for concern.

A

News articles

The project spawned several news articles and interviews. Below are multiple of these attached, along with a picture of Alex Nørgaard and I from our appearance on Go' Morgen Danmark.

Go' Morgen DK on TV2:

<https://www.youtube.com/watch?v=YS0iT8jm7lo> Peter Madsen's blog-post on Ingeniøren:

<https://ing.dk/blog/katalytisk-aktivt-besoeg-183974>

P4's interview of Alex Nørgaard:

<https://drive.google.com/file/d/0B0FJw8vW3gGmY2J5SDVlcE4zaFU/>

Figure A.1: Alex Nørgaard, Mikkel Kryger and Carl-Emil Grøn on Go' Morgen Danmark on TV2



A. News articles

view

AU Engineering news' article:

<http://ingenioer.au.dk/aktuelt/nyheder/nyhed/artikel/studerende-vil-sende-rak>

B

Rocket Logbook

Below is a logbook with directions on how the rocket was fired, along with some general firing guidelines for future groups. Several notes are found below that contain thoughts, notes and events that happened during the testing schedule.

B.1 Day 1

The test setup consists of the rocket engine with several piezoelectric and piezoresistive pressure sensors, as well as a force sensor at the back. The pressure sensors sit at various sites on the rocket, allowing us to detect any pressure waves travelling through the chamber, and measuring the rocket's pressure throughout the firing. The force sensor (henceforth mentioned as ForceLink) measures the rocket's thrust.

The equipment is set up with LabVIEW, which Gorm spent most of the first day configuring. The rocket setup was tested on day 1, otherwise, the day consisted mostly of setting up the tent and establishing a remote connection to a new computer and installing the necessary programs.

B.2 Day 2

Day 2 started early with preliminary water tests at 12:13, 12:33, 12:57 and 13:21. Two injectors, a low-flow and a high-flow, were brought



Figure B.1: Foam permeated with KMnO_4 dust inserted into the decomposition chamber, inside a tube of MDF, in order to avoid accumulation of liquid H_2O_2

along and tests of both ensued. Following the preliminary water tests, the rocket chambers were assembled and foam permeated with KMnO_4 was prepared and inserted into the decomposition chamber, as seen in figure B.1. Initial rocket test started almost two hours after the final water test at 15:20 with 1.5 L of H_2O_2 at 24 bar pressure. After the test, the stand was quite smokey as the rocket flanges were *not* tightened correctly and an O-ring was missing. A leak between the grain's chamber and the after-burn chamber seared the underside of the protective casing, thankfully without harming any of the measurement equipment. After the small upset, three additional tests were carried out.

The three first tests were all done with the low-flow nozzle with a total radius of 1.5 mm per injector hole, of which there were three. The final tests were carried out with the large injector with hole radii of 2 mm. The second test happened at 17:22 with a H_2O_2 pressure of 24 bar, the next at 18:32 with 31 bar. The final test was done at 20:19, with a H_2O_2 pressure of 31 bar, with the high-flow nozzle.

All tests were done with the same hexagonal patterned grain, with masses pre- and postburn noted.

Fixme Note: EVT. Lav tabel over tests i stedet for at skrive det

The day concluded with Peter Madsen using our test rig to test his own rocket based on a catalytic pack, with no combustion present.

The firing procedure was meticulously planned out, in order to avoid any eventual dangers. Thus, including a such list is essential for future rocketeers:

B.3 Firing Procedure

Launching the rocket requires several crucial steps in order to safely ignite the engine. Safety is the number one priority, thus, a stepwise checklist is necessary.

PRELAUNCH

1. Insert grain
2. Insert foam permeated with KMnO₄
3. Assemble rocket chambers
4. Establish remote access to control computer
5. Ensure measurement options are correct
6. Check signal and restart ManuWare
7. Create new data-log file

ALL CLEAR AREA EXCEPT FUEL RESPONSIBLE PERSON

1. Equip H₂O₂ safety equipment
2. Fill tank with H₂O₂
3. Pressurize tank
4. CLEAR THE AREA
5. Start data-collection and cameras
6. Arm the rocket
7. Fire the rocket
8. Stop data-collection and cameras
9. Remove external pressure compressor
10. Depressurize tank
11. Area is safe

B.3. Firing Procedure

Peter Madsen and his assistant Stefan Eisenknappel are the only two people present when loading the rocket with H₂O₂. The procedure is executed from start to end at each launch, and has several areas where it can be improved if time permits.

Bibliography

- [1] Bulbapedia. http://bulbapedia.bulbagarden.net/wiki/Team_Rocket, may 2016.
- [2] George P. Sutton and Oscar Biblarz. *Rocket Propulsion Elements*. Wiley, 8th edition, 2010.
- [3] Thermocouples: Using Thermocouples to Measure Temperature. <http://www.omega.com/prodinfo/thermocouples.html>, 2016.
- [4] SierraPine. *MDF Material safety data sheet*, January 2005.
- [5] Anders Hjort-Degenkolv Kristensen Alex Nørgaard, Martin Gosvig Jensen. Undersøgelse af regressionsrater i en hybrid rakettmotor, 2015.
- [6] Julio de Paula Peter Atkins. *Atkin's Physical Chemistry*. Oxford University Press, 10th edition, 2014.
- [7] John D. Clark. *Ignition!: An informal history of liquid rocket propellants*. Rutgers University Press, 1st edition, 1972.
- [8] Richard Nakka. Propellant Grain. http://www.nakka-rocketry.net/th_grain.html, july 2001.
- [9] James G. Quintiere. *Principles of Fire Behaviour*. Delmar, 1st edition, 1997.
- [10] E659-78. Standard test method for autoignition temperature of chemicals. *ASTM*, 14(5), 2000.
- [11] Nancy Hall. Compressible Area Ratio. <https://www.grc.nasa.gov/www/k-12/airplane/astar.html>, May, 2015.

Bibliography

- [12] Merle C. Potter. *Mechanics of Fluids*. 4th edition.
- [13] HorsePunchKid. De laval nozzle. https://en.wikipedia.org/wiki/Rocket_engine_nozzle#/media/File:De_laval_nozzle.svg.
- [14] Richard Nakka. Nozzle Theory. http://www.nakka-rocketry.net/th_nozz.html, April 2014.
- [15] Robert A. Braeunig. Nozzle. <http://www.braeunig.us/space/propuls.htm>, 2012.
- [16] Philip-J. Pritchard Robert W. Fox, Alan T. McDonald. *Introduction to Fluid Mechanics*. Wiley, 6th edition.
- [17] Frank M. White. *Fluid Mechanics*. McGraw-Hill Higher Education, 4th edition.
- [18] Nancy Hall. Isentropic Flow. <https://www.grc.nasa.gov/www/k-12/airplane/isentrop.html>, May, 2015.
- [19] Seppo A. Korpela. *Principles of Turbomachinery*. Wiley, 1st edition, 2012.
- [20] Steven S. Zumdahl. *Chemistry*. Houghton Mifflin, 7th edition.
- [21] Enthalpy. <http://fchart.com/ees/eeshelp/eeshelp.htm>.